

RESEARCH

Open Access



Microbial community coalescence and nitrogen cycling in simulated mortality decomposition hotspots

Sarah W. Keenan^{1*}, Alexandra L. Emmons² and Jennifer M. DeBruyn^{3*} 

Abstract

Background The pulsed introduction of dead plant and animal material into soils represents one of the primary mechanisms for returning organic carbon (C) and nitrogen (N) compounds to biogeochemical cycles. Decomposition of animal carcasses provides a high C and N resource that stimulates indigenous environmental microbial communities and introduces non-indigenous, carcass-derived microbes to the environment. However, the dynamics of the coalesced microbial communities, and the relative contributions of environment- and carcass-derived microbes to C and N cycling are unknown. To test whether environment-derived, carcass-derived, or the combined microbial communities exhibited a greater influence on C and N cycling, we conducted controlled laboratory experiments that combined carcass decomposition fluids and soils to simulate carcass decomposition hotspots. We selectively sterilized the decomposition fluid and/or soil to remove microbial communities and create different combinations of environment- and carcass-derived communities and incubated the treatments under three temperatures (10, 20, and 30 °C).

Results Carcass-derived bacteria persisted in soils in our simulated decomposition scenarios, albeit at low abundances. Mixed communities had higher respiration rates at 10 and 30 °C compared to soil or carcass communities alone. Interestingly, at higher temperatures, mixed communities had reduced diversity, but higher respiration, suggesting functional redundancy. Mixed communities treatments also provided evidence that carcass-associated microbes may be contributing to ammonification and denitrification, but that nitrification is still primarily carried out by native soil organisms.

Conclusions Our work yields insight into the dynamics of microbial communities that are coalescing during carcass decomposition, and how they contribute to recycling carcasses in terrestrial ecosystems.

Keywords Carcass decomposition, Microcosm, Nitrogen, Carbon, Biogeochemical cycling, Coalescence

*Correspondence:

Sarah W. Keenan
sarah.keenan@sdsmt.edu
Jennifer M. DeBruyn
jdebruyn@utk.edu

Full list of author information is available at the end of the article



© The Author(s) 2023. **Open Access** This article is licensed under a Creative Commons Attribution 4.0 International License, which permits use, sharing, adaptation, distribution and reproduction in any medium or format, as long as you give appropriate credit to the original author(s) and the source, provide a link to the Creative Commons licence, and indicate if changes were made. The images or other third party material in this article are included in the article's Creative Commons licence, unless indicated otherwise in a credit line to the material. If material is not included in the article's Creative Commons licence and your intended use is not permitted by statutory regulation or exceeds the permitted use, you will need to obtain permission directly from the copyright holder. To view a copy of this licence, visit <http://creativecommons.org/licenses/by/4.0/>.

Background

Animal (or carrion) decomposition results in a series of biogeochemical changes to the surrounding soil in discrete mortality “hotspots” (Carter et al. 2007; Bump et al. 2009; Benbow et al. 2019). Following deposition into an environment, carrion progress through several decomposition stages, each characterized by changes to the carcass physical and chemical properties (Keenan et al. 2019). Shortly after death, the animal’s microbiota begins decomposing internal organs and tissues (Keenan and DeBruyn 2019). During active and advanced decomposition stages, decomposition products are released into the surrounding soils as organic carbon- and nitrogen-rich fluids, along with carcass-associated microbes. The release of fluids from decomposing vertebrates alters soil physicochemical as well as biological characteristics. In particular, pH can increase or decrease, while soil electrical conductivity typically increases (Macdonald et al. 2014; Szelecz et al. 2018; Quaggiotto et al. 2019). Decomposition products stimulate micro- and macrofaunal communities (Seppey et al. 2016; Szelecz et al. 2018; Forger et al. 2019; Taylor et al. 2020), alter soil microbial community membership (Mason et al. 2023), and perturb carbon (C), nitrogen (N), and phosphorus (P) cycling for days to years (Towne 2000; Barton et al. 2016; Keenan et al. 2018a, b; Keenan et al. 2019). The input of animal-derived organic compounds provides a critical ecosystem function (Barton et al. 2019; Benbow et al. 2019; Newsome et al. 2021), and the rate at which C and N are returned to the soil and to living biomass is influenced by a wide variety of factors, including temperature (Bradford et al. 2008), moisture, soil type, and scavenging (Carter et al. 2007, 2008), all of which are challenging to control in natural ecosystems.

There are two microbial consortia implicated in C and N mineralization within mortality hotspots: (1) microorganisms from the indigenous soil environment (environment-derived) and (2) microorganisms sourced from the decomposing animal, especially the gastrointestinal tract and skin (carcass-derived) (Cobaugh et al. 2015; Hauther et al. 2015). As the animal decomposes, the carcass-derived microbes are flushed into the environment, mixing with environmental communities. Microbial community coalescence, that is, the mixing of communities, happens in various environmental scenarios, for example, mixing events in aquatic systems, soil tillage, flooding, or the introduction of exogenous organic matter (Rillig et al. 2015). In some cases, the mixing has an additive effect on community functions, with the mixed community outperforming the individual source communities. Decomposition hotspots are a zone of mixing of two very distinct microbial communities, and therefore an intriguing environment in which to understand the

ecological interaction and ecosystem consequences of microbial coalescence.

A coalesced community may comprise a mixture of the original communities, or may be dominated by one of the original communities depending on several factors, including abiotic filtering (i.e., how adapted original members are to the new environment), priority effects (i.e., who was there first), mixing ratios, interaction interfaces, temporal dynamics, and community cohesion/co-evolution (Rillig et al. 2015; Rillig and Mansour 2017; Castledine et al. 2020). Under this framework, we might expect that in mortality hotspots, carcass-derived communities would not predominate; carcass-derived microorganisms, particularly those sourced from inside an animal, are adapted to low-variability environments and may be less tolerant of temperature fluctuations and extremes. Carcass-derived microorganisms would experience pronounced abiotic filtering in the new soil environment, and priority effects would suggest soil microbes (environment-derived) might be resistant to the ‘invasion’. However, some host-associated bacteria, such as *Bacteroides*, are known to persist in surface soils well into advanced decay (Cobaugh et al. 2015; Hauther et al. 2015; Emmons et al. 2017) and up to at least four years in a sub-surface burial environment (Keenan et al. 2018a, b). In addition, many opportunistic pathogens (i.e., host-associated) have known environmental reservoirs, and display phenotypic plasticity to ensure survival in the environment (Rózsa et al. 2017). Further, carcass-derived communities have a temporal advantage over environmental microbes in that they are already actively decomposing carcass resources at the time of mixing. This suggests that host or carcass-derived microorganisms may complement environmental microbes in postmortem ecosystems and contribute to C or N cycling.

The objective of our study was to determine the effects of microbial community coalescence on biogeochemical cycling in soils in a simulated decomposition hotspot. We used laboratory microcosms to test the role of (1) environment- and carcass-derived communities and (2) temperature on C and N biogeochemical cycling in soil. A total of five treatments in triplicate were implemented to test the relative contributions of discrete microbial communities using sterile or live soil mixed with sterile or live decomposition fluids containing carcass-derived microbial communities, along with inorganic nutrient controls. The fate and transformations of C and N compounds in each of the five treatments were also evaluated under three temperatures: 10, 20, and 30 °C representing different levels of abiotic filtering. We hypothesized that a mixed or coalesced community of carcass-derived and environment-derived soil microbial communities would exhibit more rapid transformations to C and N pools

compared to communities sourced from the carcass or environment alone. Further, we expected this increase in activity in treatments held at 30 °C, as this is a temperature that would allow for greater persistence and contribution of carcass-derived microbes.

Methods

Experimental design and description

A full factorial experiment was conducted with two treatment factors: (1) microbial community, and (2) temperature, measured over time. Five microbial community treatments were designed to address whether microbial communities sourced from decomposition fluids, soil, or a combination of the two exert a greater influence on C and N cycling in a simulated decomposition system, along with control treatments with water or inorganic nutrients added (Table 1). Three temperature treatments were selected to capture a typical range for mesophiles: 10, 20, and 30 °C. The 10 and 30 °C conditions were achieved using incubators. The 20 °C microcosms were kept at ambient room temperature, which was set to 20 °C and recorded hourly using a temperature sensor (Decagon Devices, now METER Group, Inc.) to ensure consistency; the temperature was consistently at 20.4 ± 0.3 °C (range: 19.1 to 21.6 °C) for the course of the experiment. Three replicates were used for each treatment combination. All treatments were held in the dark and the experiment was conducted for 6 weeks with weekly sampling intervals.

Soil was collected on 4 November 2016, two days prior to initiating the experiment, from an agricultural test plot at the University of Tennessee East Tennessee Agriculture Research Station, Knoxville, TN (35.89708, - 83.96081). The soil was a sandy loam (59.9% sand, 23.5% silt, and 16.6% clay), classified as fine kaolinitic thermic Typic Paleudults. Soil physical, chemical, and biological properties for this location are reported in Sintim et al. (2019). Average annual temperatures in the region are 16 °C (average high = 26 °C; low = 5 °C).

Soil was sieved to 2 mm using an ethanol-sterilized (70% ethanol) sieve, removing any roots, rocks, or insects. Soil was adjusted to 7% volumetric water content using a Decagon (now METER Group Inc.) soil moisture sensor. Experiments were conducted in 946.4 mL (32 oz) wide-mouth mason jars (Ball), autoclaved before use, with a total of 45 jars (5 microbial community treatments \times 3 temperature treatments \times 3 replicates). Lids were modified to include a 20-mm-diameter chlorobutyl septa to allow for headspace gas sampling. Soil (300 g) was added to jars for treatments containing “live” soil microbial communities (Treatments 2–5) (Table 1). Soil for “carcass-derived” treatment (Treatment 1) was autoclaved four times for one hour each time, adjusted back to the appropriate soil moisture with the addition of sterile deionized water, and then placed in jars. All jars were allowed to equilibrate overnight before adding decomposition fluid or other amendments.

Decomposition fluid was collected in August 2016 from three, ~20 kg salvaged North American beavers (*Castor canadensis*). *C. canadensis* was selected as they are a common, mid-sized vertebrate in our region. Carcasses were placed into scavenger prevention enclosures (1.19 \times 0.74 \times 0.81 m) containing plastic trays to allow fluids to pool. Aliquots were collected using sterile 60-mL syringes, transferred to sterile Whirl-Pak bags, and frozen at - 20 °C until the start of the experiment. Approximately 200 mL of fluid was thawed prior to beginning the experiment.

Decomposition fluid for Treatments 1 and 3 (live carcass decomposition fluid) were directly added to soil once thawed. Fluid for Treatment 2 (soil-derived) was filtered-sterilized using a vacuum filtration apparatus to 0.22 μ m (PTFE, Corning) prior to adding to the soil. Treatment 4 consisted of soil amended with an inorganic source of ammonium, a 1 M ammonium phosphate $[(\text{NH}_4)_2\text{HPO}_4]$ solution to simulate an N-rich pulse as observed with decay fluids. A water only control (Treatment 5) tested for the effects of fluid addition to soil by adding deionized water.

Table 1 Microcosm experimental treatments. Live and sterile refer to microbial community vital state in decomposition fluid and soil

Treatment	Description	Decomposition fluid	Soil	Amendments
1	Carcass-derived	Live	Sterile	10 mL live decomposition fluid; Sterile water when needed to adjust moisture
2	Soil-derived	Sterile	Live	10 mL sterile decomposition fluid; Sterile water when needed to adjust moisture
3	Mixed carcass- and soil-derived	Live	Live	10 mL live decomposition fluid; Sterile water when needed to adjust moisture
4	Inorganic nutrient control	N/A	Live	10 mL of 1 M ammonium phosphate; Sterile water when needed to adjust moisture
5	Water control	N/A	Live	10 mL sterile water; Additional sterile water when needed to adjust moisture

After allowing soils to equilibrate overnight in their respective jars, 10 mL of the treatment fluid—live or filtered decomposition fluid, ammonium phosphate, or deionized water—was added to each jar. The volume of fluid added was designed to replicate a pulse of fluids experienced in the field during animal decomposition, without completely saturating the soils (approximately 10% volumetric water content). Fluid and soils were mixed with a sterile spatula to evenly distribute the decomposition fluids (or control fluids) throughout the jar.

Gas analyses

Initial soil gas emissions were quantified by placing a freshly collected and freshly autoclaved subsample into sterile 60 mL serum vials. Gases were collected immediately after crimping the vials (time zero) and after 24 h of incubation, providing “background” CO₂ measurements.

Volatilized gas and soil subsamples were collected weekly over the course of 6 weeks from each microcosm jar (total of 45 jars), starting after 4 days of incubation (Additional file 1: Fig. S1). During each subsampling interval, headspace CO₂ was first analyzed (0.5 mL; LI-820, Li-Cor Inc.) followed by the collection of gas (12 mL vials; Labco) for N₂O and CH₄ analyses. Vials were shipped to the University of Nebraska-Lincoln and analyzed within several weeks. The gas concentrations were quantified using an autosampler (CombiPAL; CTC Analytics, Zwingen, Switzerland) connected to a gas chromatograph (450-GC; Varian, Middleburg, The Netherlands). The GC was equipped with detectors for the measurement of CH₄ (flame ionization detector) and N₂O (electron capture detector) simultaneously.

Soil subsampling and analyses

Approximately 25 g of soil was removed weekly and separated into aliquots to characterize the N and C pools. To reduce the effects of removing soil on overall soil moisture, gas exchange between pore space and headspace, and headspace volume, each jar was initially filled with 300 g of soil. At each time point a total of ~6 g of soil was flash-frozen in sterile Whirl-Pak bags in liquid nitrogen for nucleic acid extractions, 2.5 g was air-dried for protein analyses, and ~2 g was oven-dried to quantify gravimetric moisture (mass loss after 72 h of heating at 105 °C). Total protein in soil was quantified following the Bradford Assay with the heat digestion method in duplicate (Wright and Upadhyaya 1996; Redmile-Gordon et al. 2013). Each digested sample was analyzed in triplicate following manufacturer instructions for the microplate method using a Bradford protein kit (Bio-Rad Protein Assay; Bio-Rad Laboratories). Soil electrical conductivity was measured by briefly vortexing 3 g of soil with 6 mL

of deionized water and soil pH was measured after allowing the soil slurry to settle (15 min) (Orion Star A329, Thermo Scientific).

Soil for nitrification potential analyses (2 g) was transferred to 50 mL centrifuge tubes and frozen at –20 °C until analyses. Nitrification potential was determined following a modified chlorate block method designed for a microplate reader and previously described in Keenan et al. (2018a, b). Soils for nitrification potential were incubated at the same treatment temperature by using a temperature-controlled shaking platform (for 10 and 30 °C) or shaking platform at room temperature (20 °C). Soil dissolved C and N were extracted in 0.5 M K₂SO₄ (5 g soil: 20 mL solution). After shaking for 4 h at 150 rpm at room temperature in ~230 mL (8 oz) acid-washed glass jars, the soil slurry was allowed to settle (20–30 min), vacuum filtered into 15 mL centrifuge tubes (1 µm; Ahlstrom glass microfiber filters), and stored at –20 °C until analyses for ammonium and nitrate.

Ammonium concentrations in soil extracts were measured using a modified microplate protocol (Rhine et al. 1998). Minor modifications include: (1) dissolving the ammonium standard [(NH₄)₂SO₄] in 0.5 M K₂SO₄ instead of deionized water to accommodate any potential matrix effects; (2) using 70 µL of soil extract or standard for each assay instead of 50 µL; and (3) addition of 50 µL deionized water instead of 100 µL described by Rhine et al. (1998). Absorbance of plates was measured (660 nm) after 2 h of incubation at room temperature. Nitrate was determined colorimetrically in triplicate after a 5 h incubation at room temperature following previously developed protocols (Doane and Horwath 2003).

Statistical analyses

All treatments were conducted in triplicate, allowing for averages and standard deviations to be calculated for all analyses. For statistical analyses, data were evaluated for normality using a Shapiro–Wilk test. Data were then analyzed using one-way ANOVAs to test for differences between treatments at each temperature as well as within each treatment across temperatures. Two-way ANOVAs were conducted to test for the interactive effects of time and temperature on treatment results. Post hoc testing was conducted using Tukey’s HSD test. Significance for all statistical tests was set to 0.05.

Microbial community analyses

To determine the composition of the microbial communities in the microcosms, samples reflecting key treatments and time points were selected for amplicon sequencing. Treatments 1–4 representing the different microbial community combinations and inorganic nutrients were selected, from all three temperatures (10, 20,

and 30 °C). Time points 11 and 39 days were selected to represent communities at an early and later time point in the experiment. In addition, the starting soil and decomposition fluid used in the experiment, both live and sterile, were sequenced to determine initial community composition.

DNA was extracted from soil and decomposition fluid samples using the PowerLyzer™ Power Soil DNA isolation kit (Qiagen™) per manufacturer's instructions. 0.25 g of soil and fluid were used for the extractions, and the DNA obtained after the final elution step was stored at – 20 °C until further analyses. Extracted DNA was quantified using the Quant-It™ PicoGreen™ dsDNA Quantification Kit (ThermoFisher Scientific) per manufacturer's instructions and quality of DNA was verified by 260/280 ratios in a NanoDrop™ Spectrophotometer (data not shown).

Amplicon sequencing of the 16S rRNA gene was conducted at the University of Tennessee Genomics Core Laboratory (Knoxville, TN), following their standard operating procedures of a two-step PCR. In addition to the DNA extracts from soils samples, the sequencing run also included five DNA extraction blanks (water, no soil) and one PCR blank (no template) as negative controls. As a positive control, ZymoBIOMICS Microbial Community DNA Standard (Zymo Research), which contains DNA from eight prokaryotes and two eukaryotes, was used as a template according to manufacturer's instructions for amplicon library preparation and sequencing. The V4 region of the 16S rRNA gene was amplified from extracted DNA using primers 515F GTGYCAGCMGCC GCGGTAA (Parada et al. 2016) and 806R (GGACTA CNVGGGTWTCTAAT) (Apprill et al. 2015) modified with adapters for Illumina MiSeq sequencing. The first PCR used V4 amplicon primers, Kapa HiFi master mix, and 25 cycles of PCR. The PCR product was purified with Agencourt Ampure XP beads, then each sample was indexed with a unique combination of forward and reverse Nextera XT v2, set D indexes (Illumina) using Kapa HiFi master mix, and 8 cycles of PCR. The indexed PCR product was again purified with Agencourt Ampure XP beads, and final libraries were quantified with a combination of a Nanodrop and Agilent Bioanalyzer. V4 amplicon size obtained was approximately 450 bp for the soil samples. The amplified 16S rRNA genes were sequenced at a final loading concentration of 4 pM using 250 paired-end reads on an Illumina MiSeq instrument with version 2 reagents and 15% PhiX spike-in. Raw sequence reads were deposited in the NCBI sequence read archive under BioProject PRJNA933092.

Raw sequence data were processed using mothur v.1.44.1 following the MiSeq SOP (Schloss et al. 2009). Briefly, paired reads were joined and primer sequences

removed. Reads that were of incorrect length or contained ambiguous bases were removed. Sequences were aligned to reference database (SILVA release 132) and de-noised by pre-clustering sequences with up to two nucleotide differences. Chimeras were removed using the VSEARCH algorithm. Sequences were classified using the Bayesian classifier (Wang et al. 2007) against the mothur-formatted version of the RDP PDS training set (v.9) with a bootstrap value of > 80% (Wang et al. 2007). Following this step, sequences classified as untargeted organisms (i.e., non-bacterial) were removed. Sequencing error rates were assessed by comparing the ZymoBIOMICS positive control library to a reference databases of 16S rRNA genes using the *seq.error* function in mothur. Sequences were clustered into operational taxonomic units (OTUs) based on 97% similarity. A consensus taxonomy for each OTU was generated by comparison to the RDP training set. After removing blanks, positive control, and sterile samples, the minimum library size was 44,340, therefore all libraries were rarified to this size. OTUs with only one or two reads across all samples were removed. Alpha diversity metrics (Good's coverage, Chao richness estimate, Inverse Simpson Diversity index) were calculated in mothur. The resulting alpha diversity metrics, OTU count table and taxonomy assignments were imported into R (v. 4.0.2) (R Core Team 2018) in R Studio (v. 1.3.1056) for downstream statistical analyses. Differences in alpha diversity metrics between treatments and times were determined using a three-way ANOVA with day, treatment, and temperature as factors and a post hoc Tukey HSD test to identify differences. Package Phyloseq v.1.40.0 was used for community composition visualization. Fast Expectation–Maximization for Microbial Source Tracking (FEAST) (Shenhav et al. 2019) was implemented in R (v4.2.1) (package FEAST, v0.1.0) to estimate the contributions of the carcass fluid and the soil to the communities we observed in the microcosms. Codes and associated input files are available at: <https://github.com/jdebruyne/EAGERmicrocosms>.

Bray–Curtis distances between community compositions were calculated in PRIMER v7 (Plymouth, UK) and a principal coordinate analysis (PCoA) used to visualize the differences as a function of day, treatment, and temperature. PERMANOVA was used to determine if there were statistically significant differences between communities. Initially a 3-way model was used to test for differences between day, treatment, and temperature to look for interactions, followed by pair-wise tests to determine differences between specific day, treatment, and temperature combinations.

Results

Headspace gases

Total cumulative CO₂ release, presented on a gram dry weight basis (μg C g⁻¹) (Additional file 1: Tables S1, S2, S3), was elevated for all treatments at 30 °C compared to lower temperatures (Fig. 1A), and the rate of change was also greater at 30 °C. Cumulative release at 30 °C was more than double that at 10 °C in all treatments except for Treatment 3, the mixed community. The mean cumulative CO₂ release approximately doubled for each 10 °C increase under Treatments 2 (soil-derived), 4 (nutrient control), and 5 (water control). For Treatment 1 (carcass-derived), cumulative CO₂ release declined slightly between 10 and 20 °C (85 ± 31 μg C g⁻¹ and 65 ± 43 μg C g⁻¹), but doubled under 30 °C conditions (220 ± 64 μg C g⁻¹). In Treatment 3 (mixed community), the 10 and 20 °C treatments also exhibited similar CO₂ release, which increased under 30 °C, but did not double (~150 to 250 μg C g⁻¹) (Fig. 1A; Additional file 1: Fig. S2).

At 10 °C, all treatments exhibited significant increases in CO₂ release through time, except for Treatment 3 (one-way ANOVA, post hoc testing; $p=0.432$). Treatments 1, 2, and 5 held at 20 °C did not exhibit significant change to CO₂ through time (Additional file 1: Table S3); all other treatments exhibited a significant increase in CO₂ through time. All treatments held at 30 °C exhibited significant changes to CO₂ through time.

The relative contributions of environment- and carcass-derived microbes were evaluated by comparing respiration rates (CO₂ release) between Treatments 2 and 1 (Fig. 2). The carcass-derived treatment (Treatment 1: carcass-derived) had significantly higher respiration rates compared to environment-derived microbes (Treatment 2: soil-derived) at 10 °C until day 39. At 20 °C and 30 °C the carcass-derived communities also exhibited higher respiration rates early, with soil-derived microbes increasing in relative respiration rates by day 18, particularly under 20 °C conditions.

Cumulative N₂O release over 39 days was greater in all treatments at 30 °C compared to 10 °C (all $p<0.0001$) and at 30 °C compared to 20 °C ($p<0.002$; Fig. 1B; Additional file 1: Table S4). In all treatments, except for Treatment 2, there were no significant differences in cumulative N₂O release between 10 and 20 °C ($p<0.05$). Treatment 4 exhibited the greatest cumulative release of N₂O, totaling 879.3 ± 114.6 ppm at 30 °C by day 39. In almost all treatments, except for the controls (Treatments 4 and 5), cumulative N₂O release doubled or more than doubled with each 10 °C change in temperature. In Treatment 1 (carcass only), one of the 20 °C triplicate treatments exhibited notably greater N₂O release compared to the other two jars, resulting in high standard deviations for that condition (Fig. 1B). Treatments 3 (live soil, live fluid)

and 1 (carcass-associated) exhibited similar trends and amounts of N₂O release over time (Fig. 1B; Additional file 1: Table S4). Although Treatment 3 (mixed community) tended to display greater N₂O release compared to Treatment 2 (soil alone), at no temperature was this trend statistically significant.

Methane release did not significantly differ within each treatment between the three temperatures (two-way ANOVA; $p>0.06$), except for Treatment 5 (water only), where there was a significant difference between 10 and 30 °C ($p=0.003$, $F=6.61$). At 10 °C, all treatments exhibited the significantly greater CH₄ release during days 4 and 11 (maximum value range: 2.42 ± 0.06 to 2.54 ± 0.08; one-way ANOVA; all $p<0.0001$), with a decline in subsequent sampling times. Treatments at 20 °C exhibited the same pattern (maximum value range: 2.39 ± 0.17 to 2.56 ± 0.10), except for Treatment 4, which had significantly greater CH₄ release during days 11 and 18. At 30 °C, the same pattern persists, with maximal CH₄ release during days 4 and 11. By day 39, all treatments and all temperatures had released a cumulative total of ~15 ppm CH₄ (Additional file 1: Table S5), with no significant differences between treatments or temperatures.

Soil biogeochemistry

There were significant differences in soil biogeochemistry both within and between treatments that varied as a function of temperature. Notably, soil pH increased significantly in Treatment 1 (carcass-derived) under all temperatures from days 0 and 4 compared to subsequent sampling times (one-way ANOVA; $p<0.0001$; Fig. 3, Additional file 1: Table S6), reflecting the addition of decay fluids. Treatment 2 (soil-derived) did not significantly change over time at 10 °C but exhibited significant declines at 20 and 30 °C ($p<0.001$). At 10 °C, Treatment 3 (mixed) increased from 6.28 ± 0.09 to 6.8 before decreasing over the 39 days to pH 5.78 ± 0.17. Treatment 3 at 20 and 30 °C exhibited a more rapid decline to pH ~5.5 within 11 days. Soil pH in Treatment 4 (nutrient control) followed a similar pattern as Treatment 1 at 10 °C, increasing rapidly and remaining elevated (pH ~7.5) for the duration of the experiment. In contrast, under 20 and 30 °C, Treatment 4 pH significantly declined after 11 days (both: $p<0.0001$), and continued to decrease by day 39, reaching 5.4 to 5.5. Treatment 5 (water control) did not exhibit a significant change in pH during the course of the experiment at 10 or 30 °C but exhibited significant changes at 20 °C ($p=0.0001$), decreasing from day 11 onwards.

Soil conductivity exhibited several consistent patterns across the three temperatures (Additional file 1: Table S7). Soil conductivity in Treatment 3 was greater

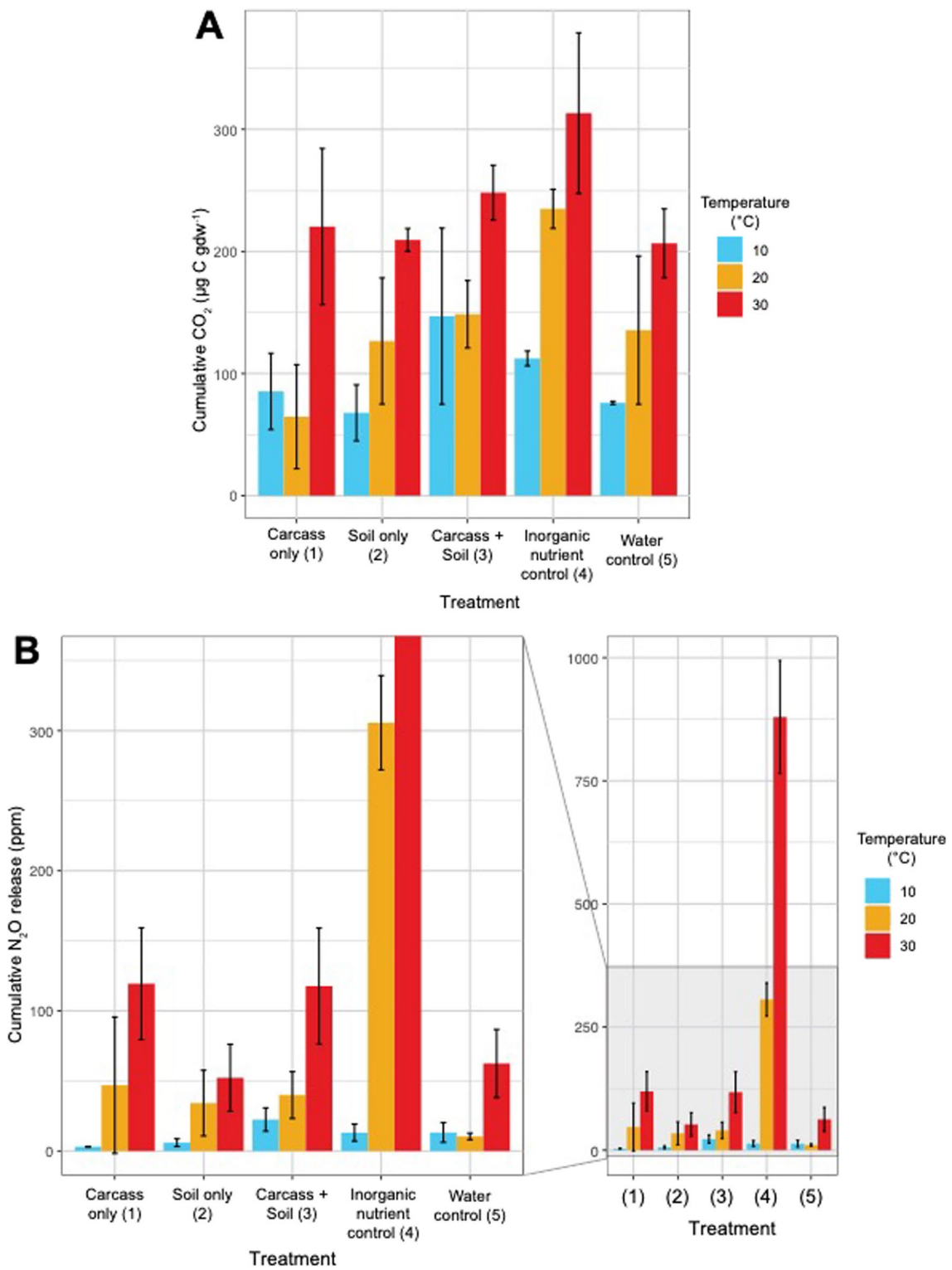


Fig. 1 Total cumulative CO₂ release (µg C g⁻¹) and N₂O release (ppm) for each treatment and temperature after 39 days. **A** CO₂ values are background-subtracted and presented on a gram dry weight. **B** N₂O release values are also background-subtracted. Both datasets represent means and standard deviations (error bars) based on technical replicates (triplicate analyses) and triplicate jars for each treatment and temperature

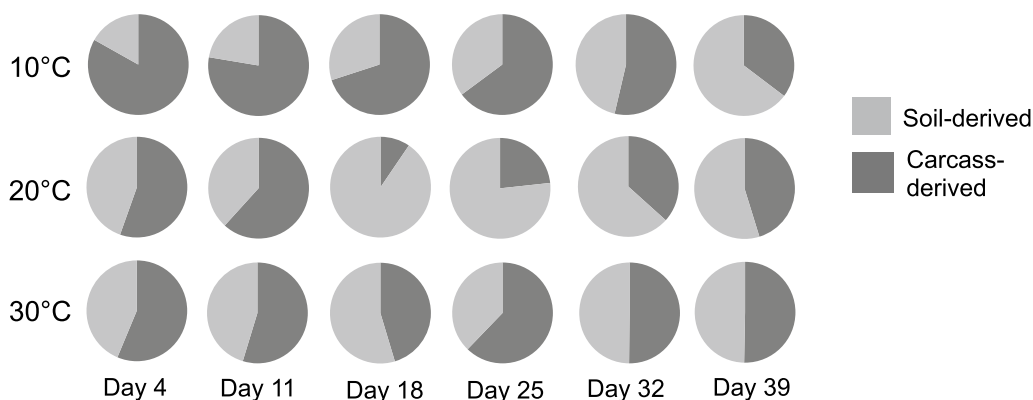


Fig. 2 Relative contributions of soil-derived (Treatment 2) and carcass-derived (Treatment 1) microorganisms to cumulative CO₂ release over time and under different temperatures

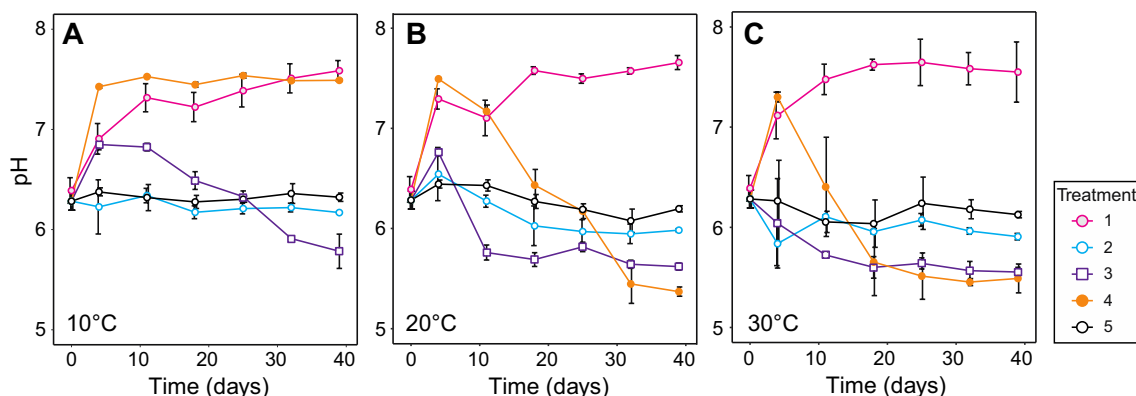


Fig. 3 Soil pH across treatments, temperatures, and over time. Treatments were held at **A** 10 °C, **B** 20 °C, and **C** 30 °C for a total of 39 days, and soils were sampled weekly. Means and standard deviations are based on triplicate experiments. Treatments are 1—carcass only; 2—soil only; 3—carcass and soil mixed; 4—inorganic nutrients control; 5—water control

than all other treatments after 11 days, except for Treatment 4, which is elevated because of inorganic N addition. Treatment 2 was the second highest in all temperatures by day 18. Treatment 1 soil conductivity did not significantly change under 10 or 30 °C but exhibited a significant decrease between days 0 and 4 at 20 °C ($p=0.002$; Additional file 1: Table S8). Treatment 5 did not change significantly at any temperature over time.

Soil ammonium and nitrate changed over time in all treatments except the water control (Fig. 4). The addition of decomposition fluids (Treatment 1 and 3) or simulated fluid (Treatment 4) between day 0 and 4 is characterized by an increase in ammonium. Ammonium remained elevated in Treatments 1 and 4 following amendment and decreased in Treatments 2 and 3 over time. Ammonium in Treatment 3 soils decreased from day 4 to 39 across all temperatures: 95 ± 17 to $42 \pm 7 \mu\text{g g}^{-1}$ at 10 °C, 106 ± 36 to 1 ± 0 at 20 °C, and 147 ± 146 to 32 ± 8 at 30 °C (Fig. 4A–C).

Nitrate increased under all temperatures in Treatments 2, 3, and 4 from day 4 through day 39 (Fig. 4D–F). Nitrate did not change significantly in Treatment 1 under 10 or 30 °C (one-way ANOVA; $p=0.11$, $F=2.162$; $p=0.19$, $F=1.72$) over time, but was elevated by $\sim 4 \mu\text{g NO}_3^- \text{N g}^{-1}$ at day 39 compared to days 32 and 25 at 20 °C ($p=0.02$, $F=3.65$). Several treatments exhibited significant changes in nitrification potential rates over time and as a function of temperature (Additional file 1: Table S9), however these changes were on the order of $0.01 \text{ mg NO}_2^- \text{ g}^{-1} \text{ day}^{-1}$, and within the range observed in other natural, untreated East Tennessee soils (Keenan et al. 2018a, b), so did not account for the large increase in nitrate observed in some treatments.

To test whether host-derived, environment-derived or combined microbial communities exerted a greater influence on changes to nitrification (ammonium to nitrate), the treatments designed to evaluate individual and

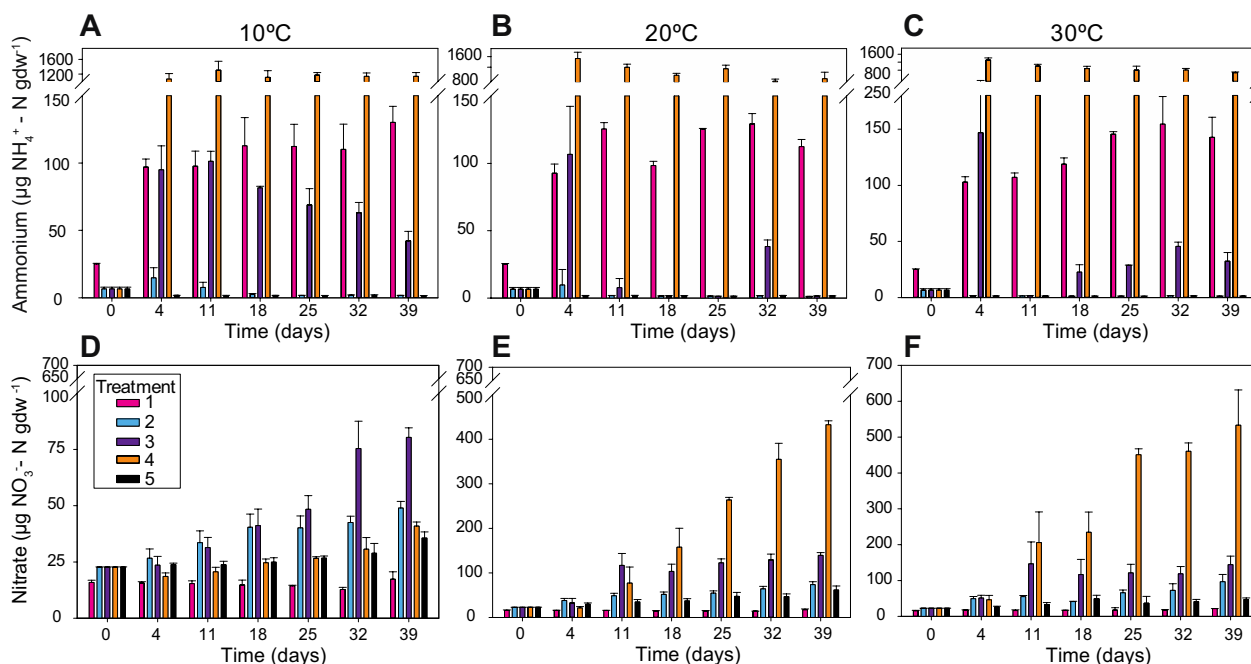


Fig. 4 Ammonium **A–C** and nitrate **D–F** concentrations in soil over time and under different temperatures. Data are presented as means ($N=3$) and standard deviations on a gram dry weight basis. Note scale change between panels. Treatments are 1—carcass only; 2—soil only; 3—carcass and soil mixed; 4—inorganic nutrients control; 5—water control

combined communities were analyzed using linear correlation analysis. Compared to soil only and carcass-only treatments, the mixed communities (Treatment 3) had greater concentrations of nitrate and exhibited a strong correlation between decreasing ammonium and increasing nitrate concentrations across all temperatures (Fig. 5).

Treatment 1 had lower protein content across all time points and temperatures compared to all other treatments, except for two times: day 25 at 20 °C and day

18 at 30 °C (Additional file 1: Tables S10, S11). Mean protein content was greater across all treatments and timepoints at 30 °C, and these differences were significant for Treatments 1, 2, 3, and for 10 °C vs. 30 °C in Treatments 4 and 5 (two-way ANOVA) (Additional file 1: Table S10). There were no consistent trends with respect to protein content changes over time or by treatment (Additional file 1: Table S11).

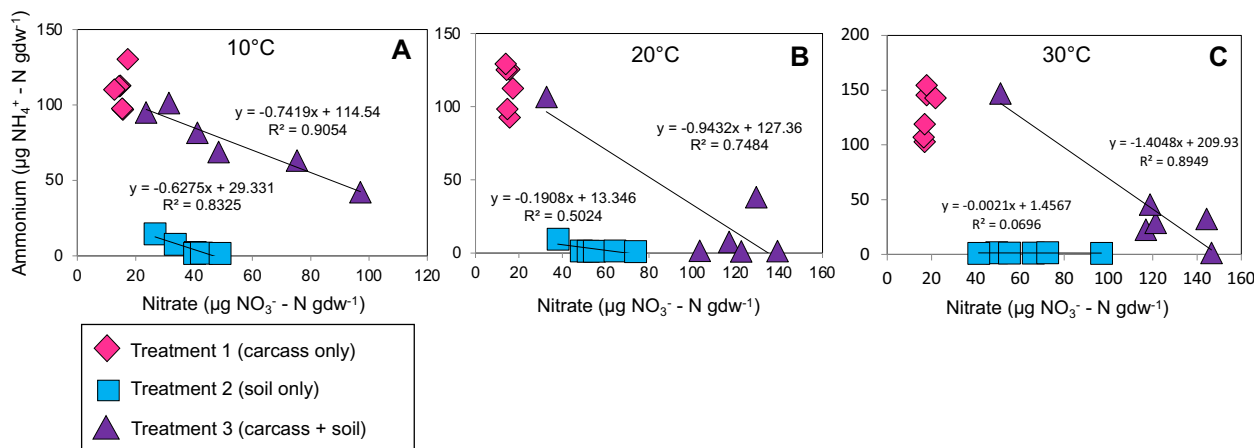


Fig. 5 Relationships between ammonium and nitrate concentration in Treatment 1 (carcass-derived), Treatment 2 (soil-derived), and Treatment 3 (mixed). The best fit linear equation for soil-derived and mixed is shown

Microbial communities: sequencing QC results

Sequencing yielded a total of 9,975,185 reads across all samples; after processing, 6,095,605 reads remained. Extraction blanks contained 49 to 120; PCR blanks contained 46 reads. The three sterile soils contained 67, 71, and 101 reads, and the three sterile decomposition fluid samples contained 106, 3128, and 9602 reads. OTUs detected in the sterile decomposition fluid were largely similar to the live fluid, albeit at reduced abundances (>90% reduction). The ZymoBIOMICS Microbial Community DNA Standard (Zymo Research) had 188,190 reads which clustered into 8 OTUs with >3 reads and identified 7 of the 8 prokaryotes in the standard (only *Staphylococcus aureus* was not detected). The sequenced Zymo sample was compared to the reference sequences using the *seq.error* function in mothur, returning an error rate of 0%. The remaining samples all had a minimum of

44,340 reads; these libraries were subsampled to the minimum size (44,340) and used for further analysis. Mean Good's coverage for the subsampled libraries was 97.64%. Sequences clustered into 10,243 OTUs with a minimum of 3 reads across all samples, with a mean of 2,656 OTUs per sample.

Microbial community composition

Carcass decomposition fluids were dominated by Firmicutes (classes Bacilli and Clostridia), with minor contributions from Proteobacteria, Actinobacteria, and Bacteroides (Fig. 6, Additional file 1: Fig. S3). In Treatment 1 (carcass only) there was a shift towards increased Proteobacteria and Bacteroides, which occurred by day 11 at the warmer temperatures and by day 39 at 10 °C (Fig. 6, Additional file 1: Fig. S3). Like Treatment 1, Treatment 4 (inorganic nutrients) also exhibited an increase

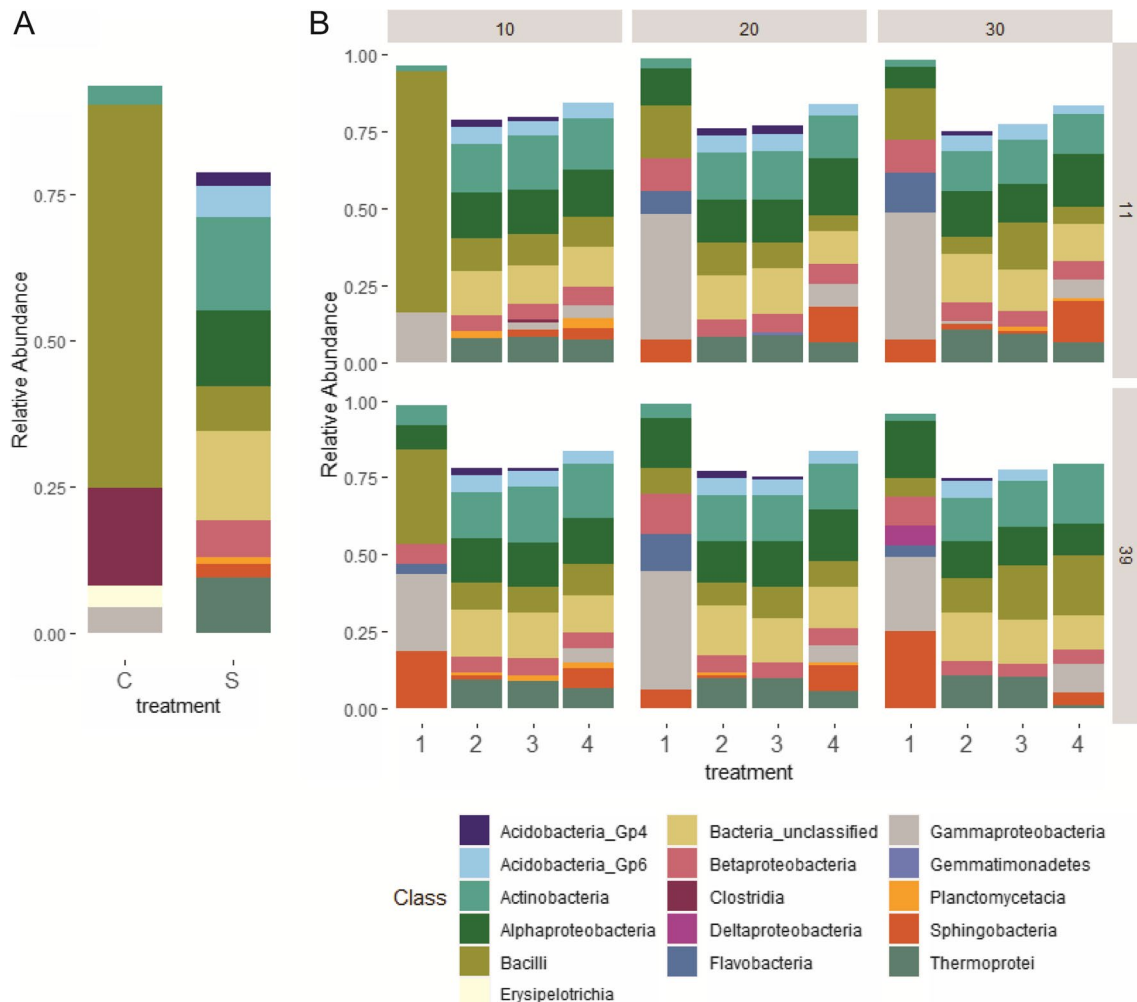


Fig. 6 Stacked bar charts showing mean ($n=3$) relative abundance of bacterial classes with a relative abundance > 1%. **A** Carcass decomposition fluid (C) and soil (S) communities at the beginning of the experiment, prior to mixing; **B** Communities in the four treatments (1—carcass derived; 2—soil derived; 3—mixed; 4—inorganic nutrients) as a function of incubation temperature (10, 20, or 30 °C) on day 11 and day 39

in the relative abundance of Proteobacteria and Bacteroides, albeit not to the extent seen in Treatment 1. In contrast, when carcass fluids were mixed with live soil (Treatment 3), we saw a decrease in Proteobacteria and Bacteroides and increase in Firmicutes (class Bacilli, but not Clostridia) relative to soil only (Treatment 2) (Fig. 6).

Alpha diversity

Initial soil samples had a high richness (mean Chao = 5815 ± 55) and diversity (mean Inverse Simpson Index = 160 ± 35) compared to all other samples (Additional file 1: Table S12). Decomposition fluids had the lowest alpha diversity (Chao = 491 ± 23 ; Inverse Simpson = 3.13 ± 0.10). Overall, Treatment 1 (carcass-derived only) had the lowest richness and diversity (mean Chao: 413 ± 12 ; Inverse Simpson = 11.6 ± 4.4), while Treatment 2 (soil only) and 3 (mixed) generally had the highest richness (overall mean Chao was 5474 ± 128 and 5323 ± 105 , respectively); Treatments 2, 3, and 4 had similar ranges of diversity (Inverse Simpson: 128.0 ± 12.8 , 105.3 ± 21.6 , and 115.0 ± 32.7 , respectively).

Testing the effect of treatment, time and temperature on Chao (richness) and Inverse Simpson (diversity) indices during the experiment, significant three-way interactions were present among all combinations of factors (Chao: $F=2.194$, $p=0.058$; Inverse Simpson: $F=2.303$, $p=0.047$). On Day 11, temperature did not have a significant effect on richness for Treatments 1, 2 and 3; for Treatment 4, 30 °C communities had significantly lower richness compared to 10 °C. Temperature did not have

a significant effect on diversity for any of the treatments on day 11. On day 39, Treatment 1 and 2 did not have a significant difference in richness or diversity between temperatures. Treatment 3 and 4 had significantly lower richness and diversity at 30 °C compared to 10 and 20 °C (Fig. 7; Additional file 1: Table S13).

Because one of our key questions was whether the mixed community (Treatment 3) would have greater diversity than the soil community alone (Treatment 2), we specifically focused on the post hoc contrasts between these two treatments. Richness was the same between Treatments 2 and 3 at all temperatures, and at both time points. Diversity, however, was different: on day 11, diversity was the same between the two treatments at 10 and 20 °C, but significantly lower in the mixed community (3) at 30 °C. On Day 39, diversity was significantly reduced in the mixed community (3) compared to soil alone (2) at both 20 and 30 °C (Fig. 7).

Beta diversity

Communities in Treatment 1 (carcass only) were very different from all the other treatments (Fig. 8A, pink symbols). All the Treatment 1 communities shifted in a similar direction away from the initial decomposition fluid communities (Fig. 8A, gray symbols), but with different magnitude based on temperature: 30 °C communities saw a bigger shift than those at 10 °C and 20 °C. When Treatment 1 is removed from the analysis, the relationships between the other treatments become apparent (Fig. 8B). A 3-way PERMANOVA using day,

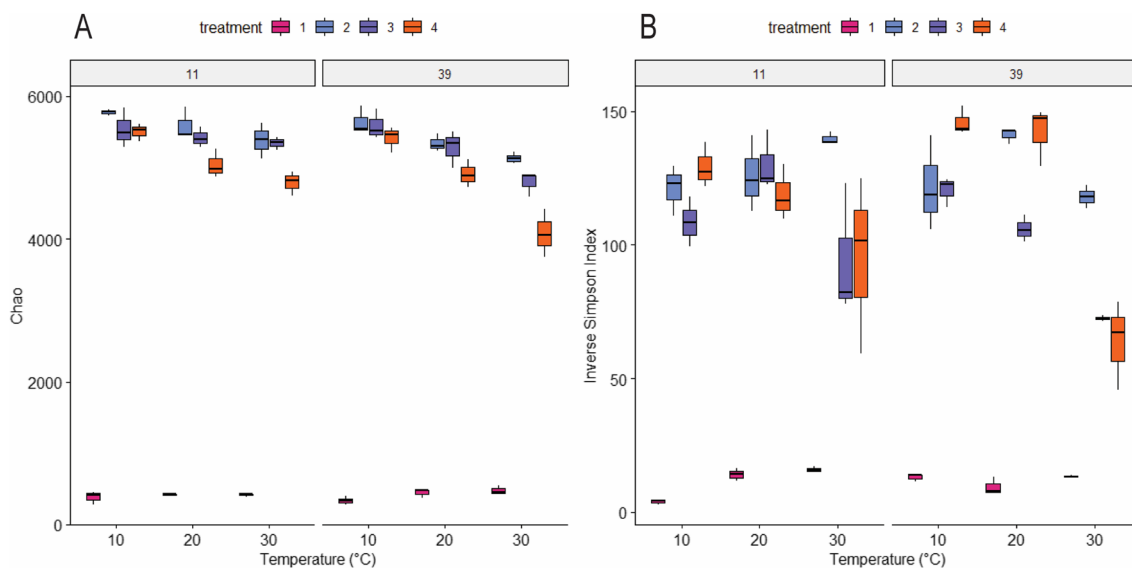


Fig. 7 Microbial community alpha diversity for all treatments (1–4), temperatures (10–30 °C), and time (day 11 and 39). **A** Richness (Chao) and **B** diversity (Inverse Simpson) of the communities on day 11 and 39 at each temperature. Treatments are 1—carcass only, 2—soil only, 3—mixed, 4—inorganic nutrients

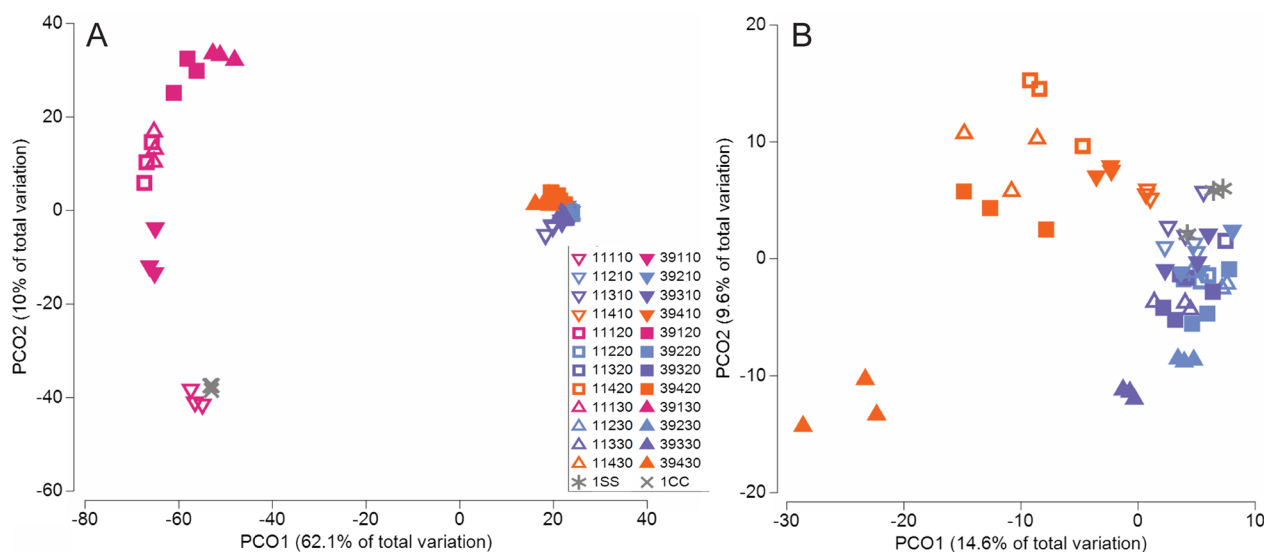


Fig. 8 Principal coordinate analyses (PCoA) of Bray–Curtis distances of bacterial communities from **A** all samples; and **B** treatments 2–4. Colors indicate treatment: pink: carcass-derived (1); blue: soil-derived (2); purple: mixed (3); orange: inorganic nutrients (4). Shapes indicate temperature: 10 °C inverted triangle, 20 °C square, 30 °C triangle. Day 11 samples are represented by open symbols and day 39 are closed symbols. Starting soil samples (1SS) are gray stars and decomposition fluid (1CC) from the carcass is represented by gray symbols. **B** PCoA of Treatments 2, 3 and 4 only. Sample names include the day (11 or 39), treatment (1–4), and temperature (10, 20, or 30 °C)

treatment, and temperature as factors identified a significant 3-way interaction (Pseudo- $F=2.326$, $p<0.001$). Subsequent pair-wise testing was used to identify significant contrasts. As with Treatment 1, Treatments 2, 3, 4 communities also changed over the course of the microcosm experiment, with the biggest changes in the 30 °C experiments. Comparing Treatment 2 (soil derived only) to Treatment 3 (mixed), both shifted away from the original soil community over time in the same general direction, towards the carcass decomposition fluid samples. At 10 °C and 20 °C, the communities in these two treatments were similar, however at 30 °C, we saw a significant difference between the two treatments, especially after day 39 (day 11: $t=1.181$, $p=0.010$; day 39: $t=1.226$, $p=0.010$). Notably, Treatment 3 (mixed) exhibited a greater shift between day 11 and 39 compared to Treatment 2 (soil derived) (Fig. 8B) and had greater similarity to the decomposition fluid samples than Treatment 2 based on hierarchical cluster analysis (Additional file 1: Fig. S4). The inorganic nutrient amended samples (Treatment 4) were significantly different from the other two.

Source tracking

FEAST was used to estimate the proportion of the communities in each microcosm that likely derived from either the carcass fluid or the soil. As expected, Treatment 1 (carcass-derived) was estimated to have the largest proportions of carcass OTUs, and Treatments 2 (soil-derived) and 4 (nutrient control) were mostly soil

OTUs (Fig. 9). In the mixed community (Treatment 3) carcass bacteria were estimated to comprise 3.4% at 10 °C on day 11 and 0.7% on day 39 (Fig. 9, Additional file 1: Table S14). At 20 °C, the carcass contribution was estimated to be 0.3% and 0.1% on days 11 and 39, respectively. At 30 °C, the carcass contribution was estimated to be 0.1% on both days.

Discussion

The mixture of carcass-associated and soil-associated microbial communities in our simulated decomposition hotspots showed that these coalesced communities behave differently than either community alone. While we might expect that carcass-associated communities would be subjected to considerable environmental filtering (i.e., not survive or thrive outside the carcass), we show that at least in some cases they were, in fact, persisting and functioning outside the host and/or impacting the native soil communities.

Effect of community mixing on C and N cycling

We observed that at 10 and 30 °C, the mixed communities exhibited greater respiration rates than either community alone, suggesting that the carcass-associated communities are adding to the soil communities' capabilities. This may be because at 10 °C, native soil organisms were slowed, reducing competition, while at 30 °C, the host-adapted carcass-microbes were likely closer to their temperature optima (i.e., 35–40 °C) (i.e., experience

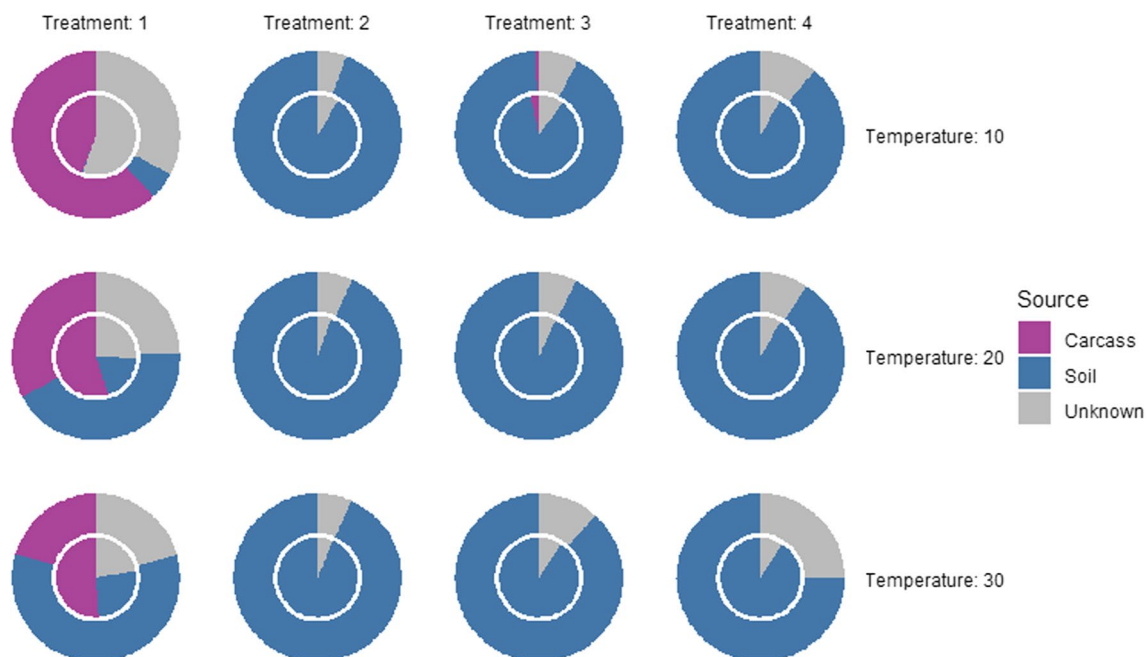


Fig. 9 Estimated proportions of the bacterial communities deriving from carcass fluid (purple) and soil (blue) generated through FEAST. Inner circle is day 11 communities, outer is day 39. Treatments are: carcass-derived (1), soil-derived (2), mixed (3), and inorganic nutrients (4). Proportions represent the means of three replicate microcosm communities

less abiotic filtering). Indeed, at 30 °C, we observed an elevated respiration response from the carcass-only treatment compared to the 10 and 20 °C incubations, indicating this was closer to their optimal temperatures. It was notable that mixing did not result in elevated respiration at 20 °C, potentially because the activity of carcass-associated microbes was reduced due to a sub-optima temperature.

In terms of nitrogen cycling, the mixed communities had similar ammonification to carcass-only communities at the beginning, suggesting that carcass-derived communities have the capacity for mineralization of organic nitrogen compounds in the decomposition environment. Midway through the incubations (day 32 at 10 °C, and day 11 at 20 and 30 °C), we observed elevated nitrate indicative of nitrification of the newly available ammonium. Nitrate production was higher for mixed communities compared to carcass- or soil-only. At 20 and 30 °C, the increase in nitrate was also observed for the inorganic nutrient addition (Treatment 4), indicating that the soil microbes are likely primarily responding to the nutrient input. However, at 10 °C, the nitrate in the mixed communities was significantly higher than what was produced from inorganic nutrients, indicating an additive or even synergistic effect; i.e., that carcass-derived microbes were also contributing to nitrification. The lack of nitrification in Treatment 1 and the elevated nitrate concentrations in Treatment 3 strongly suggests that: (1) native soil

communities play a significant role in converting ammonium to nitrate, and (2) the combined effects of native soil and host-derived microbial communities results in greater nitrification than environmental communities alone. Host-derived microbial communities are predominantly heterotrophs so we do not expect that they are conducting autotrophic nitrification directly; instead, mammalian gut members have high proteolytic capacities (Reese et al. 2018; Rowland et al. 2018), which was likely resulting in a steady supply of ammonium as substrate for the soil nitrifiers. The low nitrification potential measured in Treatment 4 may indicate that native soil communities were unable to process a large pulse of ammonium at the same rate as the lower but more steady supply of ammonium expected from microbial ammonification.

In terms of denitrification, the mixed communities had similar N₂O release compared to carcass-only communities (Fig. 1B). Altogether, our results show that carcass-associated communities were likely making contributions to ammonification and denitrification, while soil microbes were more important in terms of nitrification. Mammalian gut microbes have ammonification capabilities, such as ureolysis (e.g., Veckerskii et al. 2015), amino acid degradation (e.g., Muegge et al. 2011), and dissimilatory nitrate reduction to ammonia (e.g., Tiso and Schechter 2015). Additionally, denitrification by gut microflora has been described (e.g., Ngugi et al. 2011;

Depkat-Jakob et al. 2013). The observation that the mixed communities had equal or higher levels of activity compared to soil only or carcass-only communities suggests a cooperative or additive effect of this coalescence. This metabolic mutualism is likely not obligate, as in syntrophy (Morris et al. 2013), since both communities have members that can perform all steps of the nitrogen cycle. Rather, this is likely a situation where the more efficient members of the coalesced community come to dominate the process.

Persistence of carcass-associated microbes in soil

Using both community composition data and a bioinformatic microbial source tracking approach which estimates the proportion of each community that likely derived from a given source (in this case, our starting soil and carcass fluid communities), we saw evidence for the persistence of carcass-derived bacteria in soil. When inoculated into sterile soil, carcass-derived bacteria persisted in soil throughout the experiment. In particular, Proteobacteria became dominant in the absence of competition from native soil flora; this is not surprising, considering this phyla contains many *r*-selected or “weedy” bacterial species, and are often first responders following disturbance events (Fierer et al. 2007). When carcass fluids were inoculated into live soil (i.e., the coalesced communities), microbial source tracking (via FEAST) detected carcass-derived bacteria in the 10 °C microcosms, but not in the higher temperature microcosms. However, we did note that incubation at 30 °C resulted in a distinct microbial community structure with higher relative abundances of Firmicutes (especially Bacilli) and lower relative abundances of Proteobacteria compared to soil alone, which suggests that carcass-microbes may have persisted in these treatments as well. Since we used frozen carcasses to normalize the timing of decomposition, it should be noted that it is possible that the freezing and thawing may have had some effect on the carcass microbiome in terms of membership and/or activity.

We previously tracked human-specific *Bacteroides* genes in soils exposed to human decomposition, finding evidence of these obligate anaerobes for months and even years following active decomposition (Cobaugh et al. 2015; Keenan et al. 2018a, b). While it is unlikely that carcass-associated microbes are dominating when mixed with soil communities, it is reasonable to assume they are persisting in low abundances. The low abundances observed in our study may be due to the small volume of soil, weekly sampling, and unsaturated conditions which allowed for oxygen diffusion; in previous field studies with whole carcasses or cadavers, large volumes of decomposition fluids saturated the soil resulting

in anoxic conditions which may have enhanced the survival and activity of facultative anaerobes like Firmicutes (e.g., Keenan et al. 2018a, b). The persistence of carcass-associated bacteria in the environment is an evolutionary strategy seen in facultative pathogens, which proliferate in decomposition environments and employ survival strategies that will allow them to persist until they can find their way into their next host (Rózsa et al. 2017).

Firmicutes were the dominant members of the carcass fluid communities, primarily belonging to classes Bacilli and Clostridia. While Bacilli appeared to persist in our soils, it was interesting that Clostridia was only detectable in the 10 °C treatment on day 11. Clostridia have been noted to proliferate and dominant in the organs of decomposing carcasses, to the extent that some researchers have dubbed it the “Postmortem Clostridia Effect” (Javan et al. 2017). Further, in soils exposed to decomposition fluids, increased relative abundance of Firmicutes and Clostridia during active decomposition is frequently reported (Cobaugh et al. 2015; Singh et al. 2018; Mason et al. 2022, 2023). It was therefore somewhat surprising that Clostridia did not persist in our microcosms: while we saw Clostridia in the initial decomposition fluids (approximately 20% relative abundance), it fell to around 2% relative abundance by day 11, and <2% by day 39. This could be because the unsaturated soil conditions in our microcosm had higher oxygen diffusion compared to soils in field studies, causing death or sporulation of anaerobic Clostridia spp. and/or supporting the proliferation of faster-growing, aerobic taxa. Replicating these experiments under anaerobic conditions may help to address the role of oxygen on Clostridia survival in post-mortem soils.

Effect of mixing on bacterial diversity

We had hypothesized that mixing soil and decomposition fluid would increase the diversity of the communities, assuming an additive effect of combining two different communities. In addition, decomposition fluids are rich in a diversity of organic compounds, particularly amino acids and lipids, which are expected to stimulate a greater diversity of microbial communities over a protracted period of time compared to inorganic nutrients. We did note that communities with decomposition fluids (Treatments 2 and 3) had an overall higher richness and different community composition compared to inorganic nutrient addition (Treatment 4). However, in contrast to our hypothesis, we found that mixing communities (Treatment 3) did not result in a greater species richness, and by day 11 had reduced diversity at 30 °C and by day 39, reduced diversity at both 20 °C and 30 °C compared to soil only treatment.

The lack of increase in richness may have been due to the fact that the decomposition fluid communities were quite low in richness/diversity to begin with (about an order of magnitude lower than soils) so adding them to soils may have had limited impact on overall richness. Further, the source tracking analysis estimated that these carcass-derived communities were present in very low abundances. The decrease in diversity in the coalesced communities was more surprising. We observed that evenness was reduced due to an increase in Firmicutes (Bacilli) relative abundance and decreases in more oligotrophic phyla (Gemmatimonadetes and Acidobacteria), which suggests the introduction of the carcass communities invoked a disturbance-like response in the native soil communities. However, despite reduction of diversity in the mixed communities, it was notable that general microbial activity was not affected: respiration was either the same or higher in mixed communities compared to soil alone, particularly at 10 and 30 °C. This suggests functional redundancy in these communities.

Conclusions

Carcass-derived bacteria persisted in soils in our simulated decomposition scenarios, albeit at low abundances. Carcass-derived bacteria contributed to general community functions (carbon and nitrogen cycling), especially at temperatures closer to their optima (30 °C) when abiotic filtering is decreased, and influenced native soil community diversity. Despite the reduced diversity, the coalesced communities maintained general (respiration) activity, suggesting functional redundancy. As a consequence of mixing, coalesced communities also had higher ammonification and denitrification rates compared to soil or carcass communities alone, demonstrating that coalescence has the potential to elevate some biogeochemical processes. Surprisingly, Clostridia did not appear to persist in the soil environment, in contrast to prior studies, which may be a reflection of carcass diet and/or taxonomy (i.e., herbivorous beavers compared to omnivorous humans or pigs used in prior studies) or the aerated nature of the microcosms. Since our work was conducted using one carcass and one soil type, future studies could assess if these observations hold true for other systems. Our work yields insight into the dynamics of microbial communities that are mixing during carcass decomposition, and how they contribute to recycling carcasses in terrestrial ecosystems.

Abbreviations

C	Carbon
N	Nitrogen
ANOVA	Analysis of variance
OTU	Operational taxonomic unit

Supplementary Information

The online version contains supplementary material available at <https://doi.org/10.1186/s13717-023-00451-y>.

Additional file 1: Table S1. Cumulative CO₂ data for microcosms.

Table S2. Gravimetric moisture data for microcosms. **Table S3.** Tests for normality (Shapiro–Wilk) and results of one-way ANOVA testing for significant differences within each treatment and each temperature for CO₂ over time. **Table S4.** Cumulative N₂O data for microcosms. **Table S5.** Cumulative CH₄ data for microcosms. **Table S6.** Tests for normality (Shapiro–Wilk) and results of one-way ANOVA testing for significant differences within each treatment and each temperature for pH over time (days 0–39). **Table S7.** Soil conductivity for each treatment and temperature over time. **Table S8.** Tests for normality (Shapiro–Wilk) and results of one-way ANOVA testing for significant differences within each treatment and each temperature for conductivity over time (days 0–39). **Table S9.** Cumulative nitrification potential rate data for microcosms. **Table S10.** Tests for normality (Shapiro–Wilk) and results of one-way ANOVA testing for significant differences within each treatment and each temperature for protein over time (days 0–39). **Table S11.** Protein content of soils from each treatment and temperature over time. **Table S12.** Alpha diversity metrics of microbial communities in each library. **Table S13.** Means testing for differences in alpha diversity metrics between treatments. **Table S14.** Proportion of the communities derived from the soil and carcass fluid sources, estimated using FEAST (Fast Expectation–Maximization for Microbial Source Tracking). **Figure S1.** Schematic diagram of the sampling protocol for each microcosm jar. **Figure S2.** Cumulative CO₂ release (μg g⁻¹) across all treatments, temperatures, and over time. **Figure S3.** Stacked bar charts showing mean (n = 3) relative abundance of bacterial phyla with a relative abundance > 1%. **Figure S4.** Hierarchical clustering of group average Bray–Curtis distances, relating Treatments 2 (soil only) and 3 (soil + carcass) to the initial decomposition communities (C).

Acknowledgements

Emily Grimes and Kathleen Hauther assisted with sample collection and processing.

Author contributions

SWK and JMD designed and conducted the experiment. SWK performed the experiments, and ALE and JMD performed the sequencing and bioinformatic analyses. SWK and JMD wrote initial drafts of the manuscript, and all authors contributed to reviewing and editing the paper.

Funding

Funding for this research was provided by the National Science Foundation (Award 1549726) to JMD. Funding for open access to this research was provided by the University of Tennessee Open Publishing Support Fund.

Availability of data and materials

The sequence data generated and analyzed during the current study are archived in the NCBI sequence read archive under BioProject PRJNA933092. Data analysis codes and associated input files are available at: <https://github.com/jdebruyne/EAGERmicrocosms>. All other data are included in this published article and its supplementary information files.

Declarations

Ethics approval and consent to participate

Not applicable.

Consent for publication

Not applicable.

Competing interests

The authors declare that they have no competing interests.

Author details

¹Department of Geology and Geological Engineering, South Dakota School of Mines and Technology, 501 East St. Joseph Street, Rapid, SD 57701, USA.

²Department of Anthropology, University of Tennessee, Knoxville, TN, USA.

³Department of Biosystems Engineering and Soil Science, University of Tennessee, 2506 E.J. Chapman Drive, Knoxville, TN 37996, USA.

Received: 27 April 2023 Accepted: 6 August 2023

Published online: 11 September 2023

References

- Apprill A, McNally S, Parsons R, Weber L (2015) Minor revision to V4 region SSU rRNA 806R gene primer greatly increases detection of SAR11 bacterioplankton. *Aquatic Microbial Ecol* 75:129–137
- Barton PS, McIntyre S, Evans MJ, Bump JK, Cunningham SA, Manning AD (2016) Substantial long-term effects of carcass addition on soil and plants in a grassy eucalypt woodland. *Ecosphere* 7:e01537. <https://doi.org/10.1002/ecs2.1537>
- Barton PS, Evans MJ, Foster CN, Pechal JL, Bump JK, Quaggiotto MM, Benbow ME (2019) Towards quantifying carrion biomass in ecosystems. *Trends Ecol Evol* 34:950–961
- Benbow ME, Barton PS, Ulyshen MD, Beasley JC, DeVault TL, Strickland MS, Tomberlin JK, Jordan HR, Pechal JL (2019) Necrobiome framework for bridging decomposition ecology of autotrophically and heterotrophically derived organic matter. *Ecol Monogr* 89:e01331. <https://doi.org/10.1002/ecm.1331>
- Bradford MA, Davies CA, Frey SD, Maddox TR, Melillo JM, Mohan JE, Reynolds JF, Treseder KK, Wallenstein MD (2008) Thermal adaptation of soil microbial respiration to elevated temperature. *Ecol Lett* 11:1316–1327
- Bump JK, Webster CR, Vucetich JA, Peterson RO, Shields JM, Powers MD (2009) Ungulate carcasses perforate ecological filters and create biogeochemical hotspots in forest herbaceous layers allowing trees a competitive advantage. *Ecosystems* 12:996–1007
- Carter DO, Yellowlees D, Tibbett M (2007) Cadaver decomposition in terrestrial ecosystems. *Naturwissenschaften* 94:12–24
- Carter DO, Yellowlees D, Tibbett M (2008) Temperature affects microbial decomposition of cadavers (*Rattus rattus*) in contrasting soils. *Appl Soil Ecol* 40:129–137
- Castledine M, Sierocinski P, Padfield D, Buckling A (2020) Community coalescence: an eco-evolutionary perspective. *Philos T Roy Soc B* 375:20190252. <https://doi.org/10.1098/rstb.2019.0252>
- Cobaugh KL, Schaeffer SM, DeBruyn JM (2015) Functional and structural succession of soil microbial communities below decomposing human cadavers. *PLoS ONE* 10:e0130201. <https://doi.org/10.1371/journal.pone.0130201>
- Depkat-Jakob PS, Brown GG, Tsai SM, Horn MA, Drake HL (2013) Emission of nitrous oxide and dinitrogen by diverse earthworm families from Brazil and resolution of associated denitrifying and nitrate-dissimilating taxa. *FEMS Microbiol Ecol* 83:375–391
- Doane TA, Horwath WR (2003) Spectrophotometric determination of nitrate with a single reagent. *Anal Lett* 36:2713–2722
- Emmons AL, DeBruyn JM, Mundorff AZ, Cobaugh KL, Cabana GS (2017) The persistence of human DNA in soil following surface decomposition. *Sci Justice* 57:341–348
- Fierer N, Bradford MA, Jackson RB (2007) Toward an ecological classification of soil bacteria. *Ecology* 88:1354–1364
- Forger LV, Woolf MS, Simmons TL, Swall JL, Singh B (2019) A eukaryotic community succession based method for postmortem interval (PMI) estimation of decomposing porcine remains. *Forensic Sci Int* 302:109838. <https://doi.org/10.1016/j.forsciint.2019.05.054>
- Hauter KA, Cobaugh KL, Jantz LM, Sparer TE, DeBruyn JM (2015) Estimating time since death from postmortem human gut microbial communities. *J Forensic Sci* 60:1234–1240
- Javan GT, Finley SJ, Smith T, Miller J, Wilkinson JE (2017) Cadaver thanatomicrobiome signatures: the ubiquitous nature of *Clostridium* species in human decomposition. *Front Microbiol* 8:2096. <https://doi.org/10.3389/fmicb.2017.02096>
- Keenan SW, DeBruyn JM (2019) Changes to vertebrate tissue stable isotope ($\delta^{15}\text{N}$) composition during decomposition. *Sci Rep* 9:9929. <https://doi.org/10.1038/s41598-019-46368-5>
- Keenan SW, Emmons AL, Taylor LS, Phillips G, Mason AR, Mundorff AZ, Bernard EC, Davoren J, DeBruyn JM (2018a) Spatial impacts of a multi-individual grave on microbial and microfaunal communities and soil biogeochemistry. *PLoS ONE* 13:e0208845. <https://doi.org/10.1371/journal.pone.0208845>
- Keenan SW, Schaeffer SM, Jin VL, DeBruyn JM (2018b) Mortality hotspots: nitrogen cycling in forest soils during vertebrate decomposition. *Soil Biol Biochem* 121:165–176
- Keenan SW, Schaeffer SM, DeBruyn JM (2019) Spatial changes in soil stable isotopic composition in response to carrion decomposition. *Biogeosciences* 16:3929–3939
- Macdonald BCT, Farrell M, Tuomi S, Barton PS, Cunningham SA, Manning AD (2014) Carrion decomposition causes large and lasting effects on soil amino acid and peptide flux. *Soil Biol Biochem* 69:132–140
- Mason AR, McKee-Zech HS, Hoeland KM, Davis MC, Campagna SR, Steadman DW, DeBruyn JM (2022) Body Mass Index (BMI) impacts soil chemical and microbial response to human decomposition. *Mosphere* 7(5):e00325-22. <https://doi.org/10.1128/msphere.00325-22>
- Mason AR, Taylor LS, DeBruyn JM (2023) Microbial ecology of vertebrate decomposition in terrestrial ecosystems. *FEMS Microbiol Ecol* 99:fia006
- Morris BE, Henneberger R, Huber H, Moissl-Eichinger C (2013) Microbial syntrophy: interaction for the common good. *FEMS Microbiol Rev* 37:384–406
- Muegge BD, Kuczynski J, Knights D, Clemente JC, Gonzalez A, Fontana L, Henrissat B, Knight R, Gordon JI (2011) Diet drives convergence in gut microbiome functions across mammalian phylogeny and within humans. *Science* 332:970–974
- Newsome TM, Barton B, Buck JC, DeBruyn J, Spencer E, Ripple WJ, Barton PS (2021) Monitoring the dead as an ecosystem indicator. *Ecol Evol* 11:5844–5856
- Ngugi DK, Ji R, Brune A (2011) Nitrogen mineralization, denitrification, and nitrate ammonification by soil-feeding termites: a ^{15}N -based approach. *Biogeochemistry* 103:355–369
- Parada AE, Needham DM, Fuhrman JA (2016) Every base matters: assessing small subunit rRNA primers for marine microbiomes with mock communities, time series and global field samples. *Environ Microbiol* 18:1403–1414
- Quaggiotto MM, Evans MJ, Higgins A, Strong C, Barton PS (2019) Dynamic soil nutrient and moisture changes under decomposing vertebrate carcasses. *Biogeochemistry* 146:71–82
- R Core Team (2018) R: A Language and Environment for Statistical Computing. R Foundation for Statistical Computing, Vienna, Austria.
- Redmile-Gordon MA, Armenise E, White RP, Hirsch PR, Goulding KWT (2013) A comparison of two colorimetric assays, based upon Lowry and Bradford techniques, to estimate total protein in soil extracts. *Soil Biol Biochem* 67:166–173
- Reese AT, Pereira FC, Schintlmeister A, Berry D, Wagner M, Hale LP et al (2018) Microbial nitrogen limitation in the mammalian large intestine. *Nat Microbiol* 3(12):1441–1450. <https://doi.org/10.1038/s41564-018-0267-7>
- Rhine ED, Sims GK, Mulvaney RL, Pratt EJ (1998) Improving the Berthelot reaction for determining ammonium in soil extracts and water. *Soil Sci Soc Am J* 62:473–480
- Rillig MC, Mansour I (2017) Microbial ecology: community coalescence stirs things up. *Current Biol* 27:R1280–R1282
- Rillig MC, Antonovics J, Caruso T, Lehmann A, Powell JR, Veresoglou SD, Verbruggen E (2015) Interchange of entire communities: microbial community coalescence. *Trends Ecol Evol* 30:470–476
- Rowland I, Gibson G, Heinken A, Scott K, Swann J, Thiele I et al (2018) Gut microbiota functions: metabolism of nutrients and other food components. *Eur J Nutr* 57(1):1–24. <https://doi.org/10.1007/s00394-017-1445-8>
- Rózsa L, Apari P, Sulyok M, Tappe D, Bodo I, Hardi R, Müller V (2017) The evolutionary logic of sepsis. *Infect Genet Evol* 55:135–141
- Schloss PD, Westcott SL, Ryabin T, Hall JR, Hartmann M, Hollister EB, Lesniewski RA, Oakley BB, Parks DH, Robinson CJ, Sahl JW, Stres B, Thallinger GG, Van Horn DJ, Weber CF (2009) Introducing mothur: open-source, platform-independent, community-supported software for describing and comparing microbial communities. *Appl Environ Microb* 75:7537–7541
- Seppye CVW, Fournier B, Szelecz I, Singer D, Mitchell EAD, Lara E (2016) Response of forest soil euglyphid testate amoebae (Rhizaria: Cercozoa) to

- pig cadavers assessed by high-throughput sequencing. *Int J Legal Med* 130:551–562
- Shenhav L et al (2019) FEAST: fast expectation-maximization for microbial source tracking. *Nat Methods* 16:627–632
- Singh B, Minick KJ, Strickland MS, Wickings KG, Crippen TL, Tarone AM, Benbow ME, Sufrin N, Tomberlin JK, Pechal JL (2018) Temporal and spatial impact of human cadaver decomposition on soil bacterial and arthropod community structure and function. *Front Microbiol* 8:02616. <https://doi.org/10.3389/fmicb.2017.02616>
- Sintim HY, Bandopadhyay S, English ME, Bary AI, DeBruyn JM, Schaeffer SM, Miles CA, Reganold JP, Flury M (2019) Impacts of biodegradable plastic mulches on soil health. *Agr Ecosyst Environ* 273:36–49
- Szelecz I, Koenig I, Seppely CVW, Le Bayon RC, Mitchell EAD (2018) Soil chemistry changes beneath decomposing cadavers over a one-year period. *Forensic Sci Int* 286:155–165
- Taylor LS, Phillips G, Bernard EC, DeBruyn JM (2020) Soil nematode functional diversity, successional patterns, and indicator taxa associated with vertebrate decomposition hotspots. *PLoS ONE* 15:e0241777. <https://doi.org/10.1371/journal.pone.0241777>
- Tiso M, Schechter AN (2015) Nitrate reduction to nitrite, nitric oxide and ammonia by gut bacteria under physiological conditions. *PLoS ONE* 10:e0119712. <https://doi.org/10.1371/journal.pone.0119712>
- Towne EG (2000) Prairie vegetation and soil nutrient responses to ungulate carcasses. *Oecologia* 122:232–239
- Vecherskii MV, Kuznetsova TA, Stepan'kov AA (2015) Activity of ureolytic microorganisms in the gastrointestinal tract of the black grouse *Lyrurus tetrix*. *Dokl Biol Sci* 462:131–133
- Wang Q, Garrity GM, Tiedje JM, Cole JR (2007) Naïve Bayesian classifier for rapid assignment of rRNA sequences into the new bacterial taxonomy. *Appl Environ Microb* 73:5261–5267
- Wright SF, Upadhyaya A (1996) Extraction of an abundant and unusual protein from soil and comparison with hyphal protein of arbuscular mycorrhizal fungi. *Soil Sci* 161:575–586

Publisher's Note

Springer Nature remains neutral with regard to jurisdictional claims in published maps and institutional affiliations.

Submit your manuscript to a SpringerOpen® journal and benefit from:

- Convenient online submission
- Rigorous peer review
- Open access: articles freely available online
- High visibility within the field
- Retaining the copyright to your article

Submit your next manuscript at ► [springeropen.com](https://www.springeropen.com)
